4. Research report (Follow the guideline on the next page)

Interannual variations of SST fronts in the Peru coast

Xiaolu Tian (College of Oceanic and Atmospheric Sciences, Ocean University of China), Xinyan Mao (College of Oceanic and Atmospheric Sciences, Ocean University of China), Xinyu Guo (CMES, Ehime University)

1 Purposes

Fronts are frequently associated with highly productive regions. Due to the high productivity along the Peruvian coast, front in this region has been received extensive attention (Dengler, 1985; Vazquez-Cuervo et al., 2013; Wang et al., 2015; Yuan and Castelao, 2017). In terms of its interannual variation, Wang et al. (2021) proposed a clear negative correlation between the tropical Pacific frontal probability anomaly and the multivariate ENSO index (MEI). Frontal probability rises during La Niña years but falls during El Niño years. It revealed more about the changes in front intensity rather than the shift in front location.

In this study, we apply the Canny edge detection method to a high-resolution ocean reanalysis dataset to focus on the location of front line near the Peruvian coast, and examine the interannual location shift of the SST front, which was less mentioned in previous studies.

2 Methods

The edge detection method originated in the 1970s (e.g. Canny, 1986), and was initially used to detect image edges to determine the boundary of target. It was later applied to the detection of front line. In this study, SST fronts are identified using Canny edge detection algorithm. The edge detection algorithm has three steps involving SST gradient calculation, non-maximum suppression, and double threshold detection.

As the first step, the central difference method is used to calculate the magnitude of the SST gradient at each grid point (i, j) in the x and y directions (Eq. 1-2), where Δx and Δy represent the distances between neighboring grid points in the zonal and meridional directions, respectively. The magnitude and direction of the SST gradient vector at each

grid point are then calculated using Eq. (3)-(4).

$$Gx_{i,j} = \frac{SST_{i+1,j} - SST_{i-1,j}}{2\Delta x} \quad (1)$$

$$Gy_{i,j} = \frac{SST_{i,j+1} - SST_{i,j-1}}{2\Delta y} \quad (2)$$

$$SSTG_{i,j} = \sqrt{Gx_{i,j}{}^2 + Gy_{i,j}{}^2} \quad (3)$$

$$Dir_{i,j} = \arctan\left(\frac{Gy_{i,j}}{Gx_{i,j}}\right) \quad (4)$$

The next step, called non-maximum suppression, involves removing any grid points that are not local maximums along the direction of the gradient vector (Ren et al., 2021), which suppresses weak edge information with lower SST gradient. Following that, a final step known as double threshold detection is applied. An upper and lower threshold are specified in this step. Grid points with a gradient magnitude larger than the upper threshold are considered strong edges and flagged as front points, while those smaller than the lower threshold are removed. The other points with a gradient magnitude between the two thresholds should be further examined. If it is connected to a previously detected strong edge point, it will be also identified as a front point. This helps to improve continuity of the final front line. The two threshold values applied in this study are 5 ℃/100 km and 3 ℃/100 km, which can cover most of the SST fronts near the Peruvian coast.

3 Results

There is a long SST front band along the Peruvian coast that appears separately in three sectors: north of Lima (8°S-12°S, northern sector), between Lima and Pisco (12°S-14°S, central sector), and south of Pisco (14°S-16.5°S, southern sector). The most prominent SST fronts often occur in austral summer (Vazquez-Cuervo et al., 2013; Grados et al., 2018), and the spatial distribution of the SST fronts in summers (March) of 2006-2015 is presented here (**Fig. 1**). The southern sector is characterized by multiple frontal structures. At area south of 15°S, an obvious front extends offshore outside the upwelling front. In the summers of 2006, 2009 and 2014, the offshore front line is at approximately 15.5°S

and has a zonal distribution. In 2010 and 2011, it was found at about 16°S. However, in summers of 2013 and 2015, the angle between the offshore front and the shoreline drops to about 30°, with the northernmost part of the front reaching about 15°S. In the northern sector, SST fronts are more marked in the summers of 2009 and 2015, with a gradient of 7-9 ℃/100 km. Meanwhile, the front line position suggests that the front can move offshore or even separate from the coast, e.g. in 2009 and 2015.

SST fronts near the Peruvian coast are mainly controlled by the upwelling that caused by alongshore wind in traditional opinion. However, wind field is hardly related to interannual front location shift in comparison with mesoscale eddies. In the southern sector, the interannual meridional shift of the offshore SST front is closely connected with the north-southward movement of warm eddy in summer. In the northern sector, the separation of upwelling-induced front from the coast is likely caused by the presence of near-shore anticyclonic eddies.

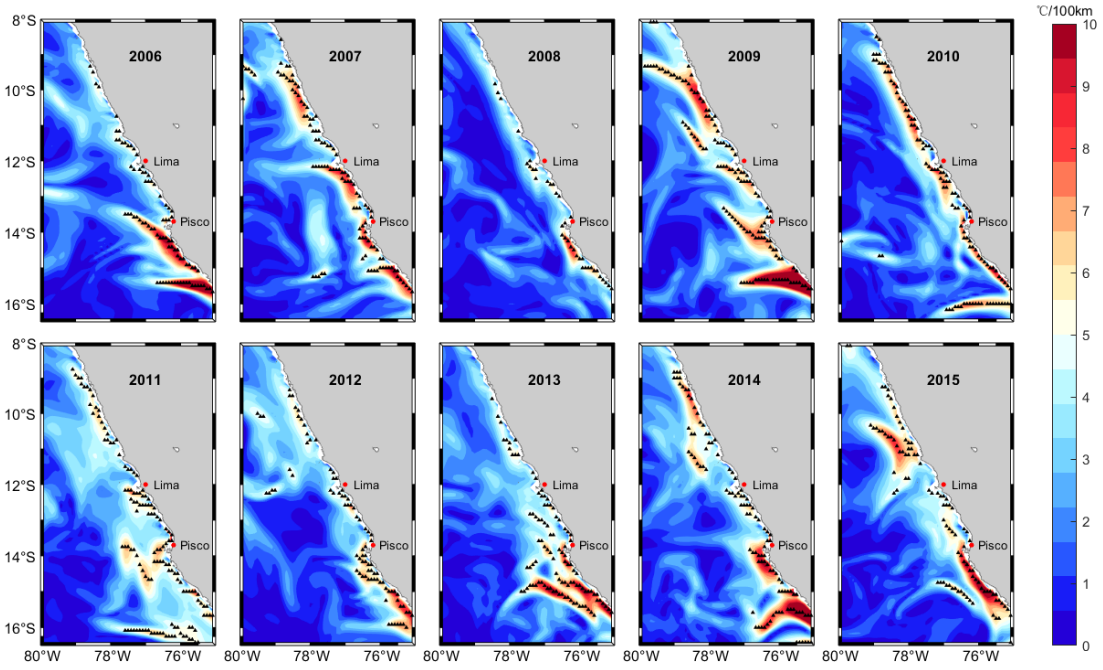

Fig. 1. Spatial distribution of SST gradient magnitude (℃/100 km) in the summer of 2006-2015. The black triangles dote the position of the SST front points identified by the edge detection algorithm. Major cities are labeled by red dots.

Fig. 2 shows the change in two front parameters detected by the edge detection method to further demonstrate the frontal interannual variability, especially in austral summer. In

the northern sector (**Fig. 2a**), the SST front intensity is higher in years of 2009, 2010, 2014 and 2015, but lower in years of 2008, 2011, 2012 and 2013. In the southern sector, the abnormal SST fronts occur in 2006, 2009 and 2014 (**Fig. 2b**), with its intensity anomaly being over +2 ℃/100 km in late summer of 2006 and 2009.

Another factor of SST front is the length of front line, which can be reflected by the number of SST front points. As illustrated in **Fig. 2c**, years with more front points correspond to the years with stronger SST front in the northern sector (**Fig. 2a**), especially in the summers of 2009 and 2015. In 2009, for example, nearly 40 more front points were detected than average year, indicating a relatively longer front line, which agrees well with the higher front intensity at that time. In the southern sector (**Fig. 2d**), longer front lines approximately correspond to longer duration of the front but not in front magnitude. There is little difference (less than 5 front points) between the remarkably strong years (e.g. 2006) and normal years. In a word, the SST front is so complicated that it cannot be completely described by a single factor, either front intensity or front points.

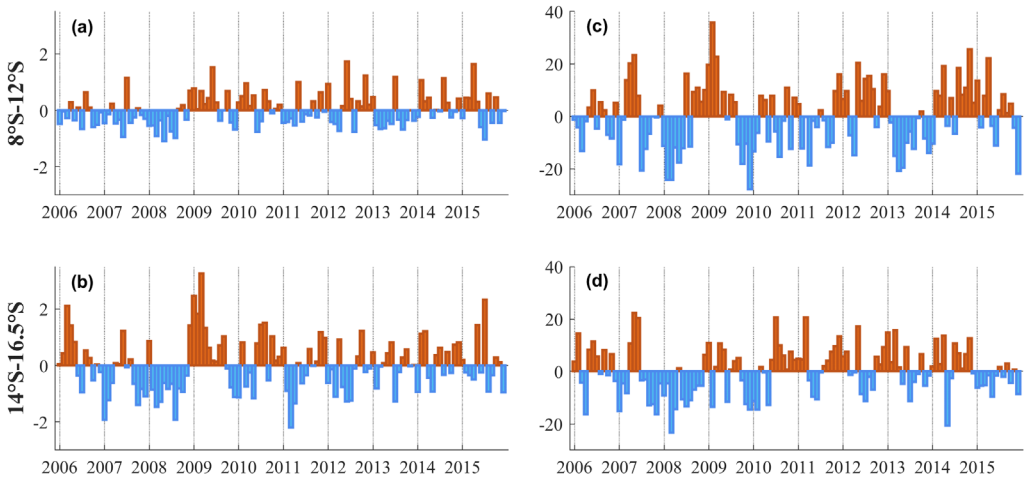

Fig. 2. Time series of (a-b) spatially average SST front intensity anomaly (℃/100 km) and (c-d) SST front points number anomaly in the northern (upper panel) and southern sector (lower panel) from 2006 to 2015.

4 Future challenges

The results showed that the offshore SST front in the southern sector has a meridional position change of around 1° among the years. And in the northern sector, the coastal SST

front detaches from the coast around 9°S-10°S and extends offshore or even completely separates from the shore in some years, while it clings to the shoreline in other years (**Fig. 1**). The mechanism of the SST front inter-annual variation has been discussed with wind and mesoscale eddies, and further dynamic discussion will be conducted in the future studies.

References

Canny J. 1986. A computational approach to edge detection. *IEEE Transactions on Pattern Analysis and Machine Intelligence*, 8(6), 679-698.

Dengler A T. 1985. Relationship between physical and biological processes at an upwelling front off Peru, 15°S. Deep Sea Research Part A. Oceanographic Research Papers, 32(11), 1301-1315.

Ren S H, Zhu X M, Drevillon, M, et al. 2021. Detection of SST Fronts from a High-Resolution Model and Its Preliminary Results in the South China Sea. Journal of Atmospheric and Oceanic Technology, 38(2), 387-403.

Strub P T, James C. 2000. Altimeter-derived variability of surface velocities in the California Current System: 2. Seasonal circulation and eddy statistics. Deep Sea Research, Part II, 47, 831-870.

Vazquez-Cuervo J, Dewitte B, Chin T M, et al. 2013. An analysis of SST gradients off the Peruvian Coast: The impact of going to higher resolution. Remote Sensing of Environment, 131, 76-84.

Wang Y T, Castelao R M, Yuan, Y P. 2015. Seasonal variability of alongshore winds and sea surface temperature fronts in Eastern Boundary Current Systems. Journal of Geophysical Research: Oceans, 120(3), 2385-2400.

Wang, Y., Liu, J., Liu, H., Lin, P., Yuan, Y., & Chai, F. 2021. Seasonal and interannual variability in the sea surface temperature front in the eastern Pacific Ocean. Journal of Geophysical Research: Oceans, 126, e2020JC016356.

Yuan Y P, Castelao R M. 2017. Eddy-induced sea surface temperature gradients in Eastern Boundary Current Systems. Journal of Geophysical Research: Oceans, 122(6), 4791-4801.